Methods and Applications in Fluorescence

PAPER • OPEN ACCESS

Linker length affects photostability of protein-targeted sensor of cellular microviscosity

To cite this article: Markéta Kubánková *et al* 2019 *Methods Appl. Fluoresc.* **7** 044004

Methods and Applications in Fluorescence

PAPER

Linker length affects photostability of protein-targeted sensor of cellular microviscosity

Markéta Kubánková[1], **Joseph E Chambers**[2,5], **Roland G Huber**[3], **Peter J Bond**[3,4], **Stefan J Marciniak**[2] and **Marina K Kuimova**[1,5]

[1] Department of Chemistry, Imperial College London, Wood Lane, London, W12 0BZ, United Kingdom
[2] Cambridge Institute for Medical Research (CIMR), Department of Medicine, University of Cambridge, The Keith Peters Building, Hills Road, Cambridge, CB2 0XY, United Kingdom
[3] Bioinformatics Institute (BII), Agency for Science, Technology and Research (A*STAR), Matrix 07-01, 30 Biopolis Street, 138671 Singapore
[4] Department of Biological Sciences, National University of Singapore, 14 Science Drive 4, 117543 Singapore
[5] Authors to whom any correspondence should be addressed.

E-mail: jec202@cam.ac.uk **and** m.kuimova@imperial.ac.uk

OPEN ACCESS

RECEIVED
23 July 2019

REVISED
12 September 2019

ACCEPTED FOR PUBLICATION
26 September 2019

PUBLISHED
10 October 2019

Keywords: photostability, viscosity sensor, molecular rotor, FLIM, genetically targeted sensor

Supplementary material for this article is available online

Abstract

Viscosity sensitive fluorophores termed 'molecular rotors' represent a convenient and quantitative tool for measuring intracellular viscosity via Fluorescence Lifetime Imaging Microscopy (FLIM). We compare the FLIM performance of two BODIPY-based molecular rotors bound to HaloTag protein expressed in different subcellular locations. While both rotors are able to penetrate live cells and specifically label the desired intracellular location, we found that the rotor with a longer HaloTag protein recognition motif was significantly affected by photo-induced damage when bound to the HaloTag protein, while the other dye showed no changes upon irradiation. Molecular dynamics modelling indicates that the irradiation-induced electron transfer between the BODIPY moiety and the HaloTag protein is a plausible explanation for these photostability issues. Our results demonstrate that binding to the targeted protein may significantly alter the photophysical behaviour of a fluorescent probe and therefore its thorough characterisation in the protein bound form is essential prior to any *in vitro* and *in cellulo* applications.

1. Introduction

Within the complex and crowded intracellular milieu, microscopic viscosity (microviscosity) is a key determinant of diffusion and is predicted to influence many biological processes, including enzyme-driven metabolism and protein folding [1]. As such, there has been a surge in recent efforts to develop microviscosity sensors for the intracellular environment. Researchers have utilised a group of small molecules termed molecular rotors, which possess specific microviscosity sensitive fluorescent properties [2–4]. The properties of rotors can be calibrated in carefully chosen systems of varied viscosity outside the cell. Furthermore, ratiometric and fluorescence lifetime-based molecular rotors show signals that are independent of the probe's concentration and, therefore, can be used for quantitative viscosity measurements. Hence, fluorescence lifetime imaging (FLIM) or ratiometric fluorescence microscopy can be performed in live biological systems, where the concentration of the probe is unknown, in order to extract quantitative and spatially resolved information about the microviscosity of the probe's environment. Several molecular rotors used passive organelle localization [5–9] or genetic targeting [10, 11] to create maps of viscosity distribution within cellular organelles. These efforts have revealed that intracellular microviscosity varies greatly between distinct subcellular compartments [12].

Among the variety of molecular rotors, boron-dipyrromethene (BODIPY) based rotors are popular for viscosity studies in live cells [9, 12–15]. The advantages of BODIPY-based rotors include mono-exponential time-resolved fluorescence decays in homogeneous media, a large dynamic range of

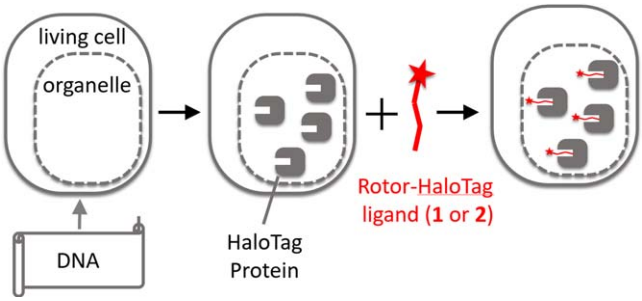

Figure 1. Schematic diagram of the genetic targeting of molecular rotor-HaloTag ligands into specific subcellular compartments. In this image, DNA represents the HaloTag expression construct instructing the cell to express HaloTag protein in the organelle of choice. The cells expressing HaloTag protein are then incubated with HaloTag ligand (in this study a conjugate of a HaloTag ligand and a molecular rotor BODIPY). The molecular rotor-HaloTag ligand internalises and binds into the active site channel of HaloTag protein.

fluorescence lifetimes in the cell-relevant viscosity range [13], temperature-independent photophysics [16] and permeability across cell membranes [13]. Targeting of BODIPY-based rotors into a desired intracellular location for real-time microviscosity determination may be achieved by rational probe design or by genetic targeting. Genetic targeting has gained popularity in the past years, as it enables directly comparable, organelle specific microviscosity measurements, revealing biophysical differences between cellular compartments [10–12]. However, genetic targeting relies on establishing a covalent link between the probe and the targeted protein, which in the case of molecular rotors may induce changes to the probe's photophysics. The increased complexity of the protein-probe system requires careful characterisation *in vitro* and *in cellulo*.

We have recently reported a HaloTag BODIPY-based molecular rotor useful for fluorescence lifetime-based (FLIM-based) measurements of intracellular viscosity in the ER, mitochondria and cellular cytoplasm [12]. In an effort to expand the range of rotors available, we have now synthesised a new BODIPY derivative for cellular targeting, which possesses a longer haloalkane chain for targeting the active site channel of HaloTag protein. Our rationale was that the altered accessibility of the rotor to the intracellular milieu can result in an altered viscosity response, e.g. a different dynamic range for our measurements. Instead, we found that the change in the linker's length is detrimental to the probe's photostability. This manuscript details our investigations into the photostability of these targeted rotor derivatives.

2. Results

2.1. The design and synthesis of molecular rotor-HaloTag ligands

In order to direct molecular rotors into specific environments within living cells, the HaloTag protein tag system was chosen, which uses genetically encoded HaloTag proteins designed to covalently bind to synthetic haloalkane ligands [17]. In addition to proprietary fluorescent HaloTag ligands, reactive linkers are commercially available and can be used to covalently link the HaloTag enzymatic substrate to fluorescent dyes, in our case a BODIPY molecular rotor. Under general physiological conditions, a covalent bond forms between the HaloTag fusion protein and HaloTag ligand's reactive linker at amino acid D106. Transfecting cells with a HaloTag expression vector and treating them with a HaloTag ligand results in the accumulation of the probe with cytosolic distribution in transfected cells. In addition, we used constructs that allowed us to direct the probe into specific subcellular compartments [12]. The principle behind the genetic targeting of molecular rotor-HaloTag ligands into specific cellular compartments is explained in figure 1. The ligands used in the study were designed in such a way that the molecular rotor moiety protrudes from the active site channel of the HaloTag protein, in order to probe the microviscosity of the surrounding microenvironment.

Two haloalkane conjugates of BODIPY were explored as molecular rotors for microviscosity sensing (figure 2), generated by reacting an N-hydroxysuccinimide (NHS) ester of BODIPY with commercially available HaloTag substrate linkers (figure S1 is available online at stacks.iop.org/MAF/7/044004/mmedia). Linkers differed in length by 2 PEG units (approximately 5.6 Å) [18], altering the eventual position of the BODIPY head group in relation to the HaloTag protein active site tunnel upon binding (figure 3, and supplementary movies 1–2). Herein these ligands are referred to as **1** and **2** (figure 2). With a longer linker, we hypothesised that the molecular rotor moiety would be located further away from the protein's surface, and therefore could potentially be less affected by the local environment e.g. non-covalent interactions with amino acids of the HaloTag protein or with its surface-associated water. Hence, different lengths of a HaloTag-targeting chain may result in a different dynamic range of sensitivity of BODIPY's fluorescence lifetimes to the microviscosity

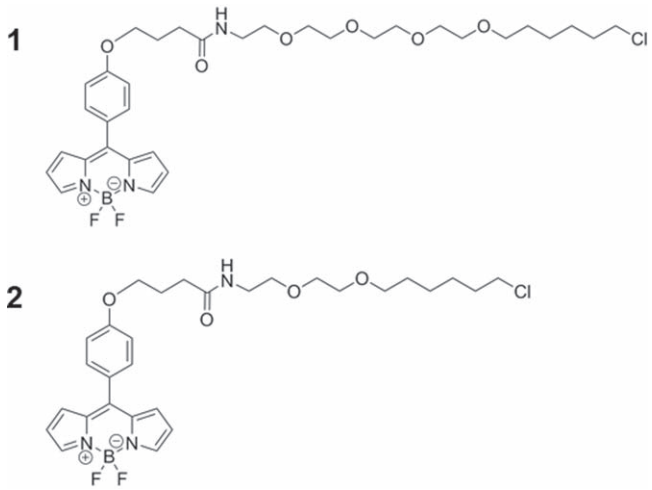

Figure 2. Molecular structures of the two BODIPY-HaloTag ligands.

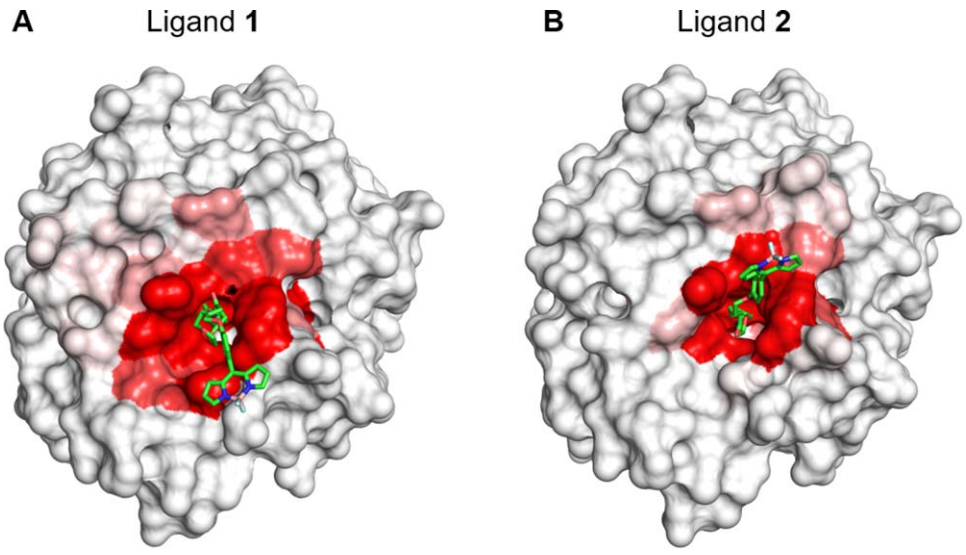

Figure 3. Computational models showing the anchoring of BODIPY-HaloTag ligands **1** (A) and **2** (B) to D106 in the channel of HaloTag protein. The contact map of the protein surface residues with BODIPY is shown in red, with brighter colour corresponding to more frequent contact, revealed during molecular dynamics simulations. It is apparent that the longer linker in **1** interacts with a broader range of residues on the HaloTag protein surface, whereas the short linker in **2** confines the rotor to a more restricted area.

of their environment. In potential future applications, the variation in dynamic ranges of lifetime responses in such rotors may be useful for more precise micro-viscosity imaging, responding to a particular range of microviscosity in different organelles of interest, which can show wide variations in microviscosity [12].

To test the feasibility of using these protein-bound probes in cells, molecular dynamics (MD) simulations were first run to explore the effect of linker length on BODIPY head group rotation in simple small solute solutions of known microviscosity (figure 3). The longer linker of probe **1** afforded the BODIPY head group a broader range of potential interactions on the HaloTag protein surface and resulted in marginally lower rotational dynamics compared with **2** (figure 3, supplementary movies 1–2).

2.2. *In vitro* characterisation of viscosity sensitivity of BODIPY-HaloTag ligands

In order to provide a quantitative measurement of viscosity using a molecular rotor, it is necessary to perform a calibration measurement of fluorescence lifetimes of the probe in simple mixtures of solvents (e.g. glycerol and water) with known viscosity values. Conventionally, the calibration data for molecular rotors can be fitted using the Förster-Hoffmann equation, which assumes the power law dependence of the fluorescence parameter (quantum yield, fluorescence lifetime or a ratio) on viscosity [19]. The $\log(\tau)$ versus $\log(\eta)$ plot should yield a straight line. This means that the viscosity measurement becomes less sensitive at higher viscosities, i.e. a smaller change in lifetime corresponds to a large change in viscosity.

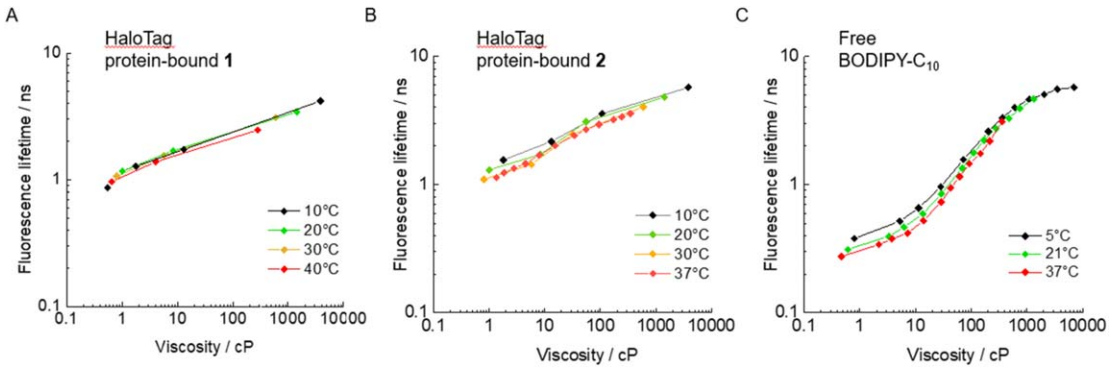

Figure 4. A comparison of the lifetime-viscosity calibrations of BODIPY-HaloTag **1** (A), BODIPY-HaloTag **2** (B) and free BODIPY-C_{10} (C) in water-glycerol mixtures at different temperatures. Average fluorescence lifetime derived from the bi-exponential decays of BODIPY-HaloTag **1** and **2** are reported (A), (B), mono-exponential fitting was performed for BODIPY-C_{10} (C). A decreased dynamic range of fluorescence lifetime is apparent for protein-bound **1** and **2**, compared to the free BODIPY-C_{10}. The calibration curves recorded at variable temperature display a high degree of overlap, demonstrating that the temperature sensitivity is relatively small in all cases. Data shown in B and C were reproduced with permission from [12].

To create a calibration system with properties matching the *in cellulo* measurement system, it was important to calibrate protein-bound ligands (herein referred to as BODIPY-HaloTag **1** and **2**), rather than simply calibrating the unbound ligands. For this reason, we purified HaloTag protein and incubated it with **1** and **2** to create protein-bound systems for *in vitro* calibration purposes.

Water-glycerol mixtures of different viscosities were previously used for the calibration of BODIPY-HaloTag **2** [12]; here we compare these results to the water-glycerol calibration of BODIPY-HaloTag **1**. The fluorescence decays of the protein-bound ligands were recorded as a function of solvent viscosity at a fixed temperature. In both cases the decay constants became longer with increasing viscosity, confirming the viscosity-sensing ability of BODIPY-HaloTag **1** and **2** (figure S2). The decays were non mono-exponential even in this relatively simple system of water-glycerol mixtures, consistent with previously reported data for BODIPY-HaloTag **2**, and were best fitted with a bi-exponential model. The linear relationship between $\log(\tau)$ and $\log(\eta)$ at higher glycerol concentrations argues strongly against aberrant effects of glycerol on the folded state of HaloTag. The measurements were repeated at variable temperature (10 °C–40 °C) to test the sensitivity of the rotor responses to the environmental temperature, which may be important for the cellular viscosity measurements, often performed at physiological temperature of 37 °C.

The average lifetime-viscosity calibration plots of BODIPY-HaloTag **1** and **2** in water-glycerol mixtures are shown in figures 4(A) and (B), respectively. Both exhibit a relatively similar response of fluorescence lifetime to viscosity and the overlap of calibration curves at different temperatures rules out any significant temperature sensitivity of the probes. In calibration mixtures of viscosities ranging between *ca* 1–7000 cP, the dynamic range of the average fluorescence lifetime of both ligands is *ca* 1–5.7 ns (figures 4(A) and (B)). These calibration curves can be contrasted to the calibration plot of free BODIPY-C_{10} (figure 4(C), molecular structure shown in figure S1(C)). From this comparison it is clear that the protein-bound probes have a narrower dynamic range compared to the free probe. The main difference appears at the lower limit of viscosity/lifetime, as the fluorescence lifetimes of protein-bound **1** and **2** do not reach below 1 ns, compared to *ca* 0.3 ns for the free BODIPY-C_{10}. We attribute this fact to the presence of bulky HaloTag protein causing steric hindrance to the rotors, which then cannot rotate as freely, resulting in a higher fluorescence lifetime. These results are in line with what was previously observed for covalently bound molecular rotors: a reduced dynamic range of lifetime versus viscosity calibration of BODIPY- and cyanine-based rotors was detected upon covalent attachment of rotors to a solid surface [20] or to various proteins undergoing amyloid assembly [14].

These data indicate that, within experimental error of our measurements, protein-bound **1** and **2** have nearly identical dynamic ranges of lifetimes in response to viscosity, indicating that the length of the HaloTag binding motif does not significantly affect their exposure to the solvent environment and the intramolecular rotation that results. We also recorded a minimal sensitivity of the sensors' responses to the environmental temperature, which makes both these probes applicable for measurements at variable temperature (i.e. between 10 °C–37 °C in live cells).

2.3. Linker length affects photostability of BODIPY-HaloTag ligands

Having confirmed the viscosity sensitivity of BODIPY-HaloTag **1** and **2** and performed lifetime-viscosity calibration measurements, we proceeded to cell studies. We have previously reported that **2** is suitable for imaging microviscosity in the ER, mitochondria, cell nucleus and cell cytoplasm [12]. As expected from

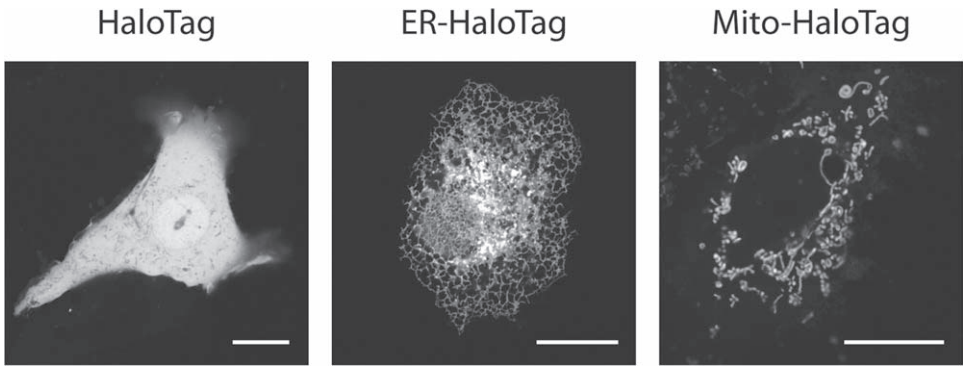

Figure 5. Localisation of **1** in COS7 cells expressing HaloTag protein in the cytosol (HaloTag, left), HaloTag containing an N-terminal signal sequence and a C-terminal KDEL motif that localised to the endoplasmic reticulum (ER-HaloTag, centre), and HaloTag containing the N-terminal mitochondrial targeting sequence of human cytochrome oxidase 8 A that localised to the mitochondrial matrix (Mito-HaloTag, right). Images were acquired using a Zeiss LSM780 confocal microscope using an excitation wavelength of 488 nm. 20 μm scale bars are inset.

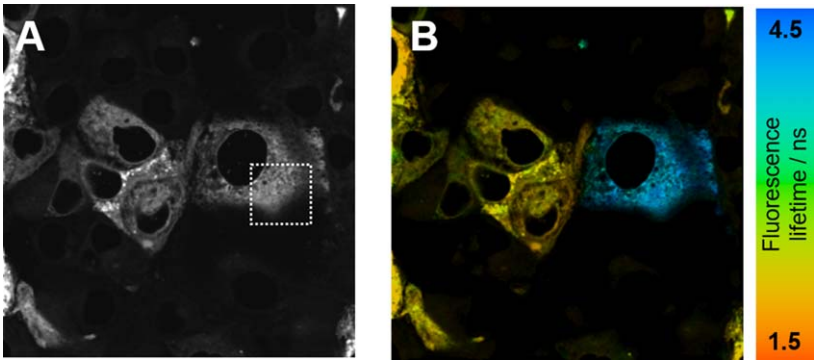

Figure 6. Two photon intensity (A) and FLIM (B) images of COS7 cells stained with ligand **1** following the irradiation of a small region of a cell using 930 nm excitation at 2 mW for 5 min. The irradiation of a small region (shown as a white dashed rectangle in A) resulted in the increase of the fluorescence lifetime of **1** in the whole affected cell, while the surrounding cells maintained the original fluorescence lifetime.

HaloTag targeting, **1** showed a good localisation to the ER, mitochondria, cell nucleus and cell cytoplasm (figure 5). Surprisingly, we observed that when a sequence of fluorescence lifetime images was recorded from the same field of view of cells, the fluorescence lifetime of **1** increased in each image, in the absence of any external stimuli (figure 6). The higher the laser power, the more significant the fluorescence lifetime changes of BODIPY-HaloTag **1**, a trend that was not observed with BODIPY-HaloTag **2**. The highest observed photo-induced increase of fluorescence lifetime was in the range of nanoseconds, an extremely high value considering the dynamic range of the probe. In contrast, when **2** was tested under similar conditions for possible irradiation induced effects, the fluorescence lifetime of BODIPY-HaloTag **2** remained stable even after 15 min of irradiation at the highest power used (figure S3).

In all experiments, the multiphoton excitation laser power was kept to a minimum in order to prevent phototoxicity to the imaged cells and was not more than 1–2 mW (measured at the microscope stage), which is generally considered to be well within the 'safe zone' for imaging live cells using near-infrared femtosecond irradiation [21] and when using standard fluorophores such as Fluorescein or GFP, which are not efficient at producing reactive oxygen species [22]. A gradual increase of fluorescence lifetime of BODIPY-HaloTag **1** was observed even upon excitation with low laser power (figure 7(A)), with a lifetime increase in the range of 0.1–0.3 ns over standard imaging time and conditions. Along with the corresponding lifetime increase, practical use of the probe in cells was precluded by extremely low fluorescence intensity at such low excitation powers, resulting in very long acquisition times, hampering the investigation of fast dynamic processes.

Our previous work highlighted a range of viscosity values detected in various cell organelles, e.g. 35 and 56 cP in the cytosol and the nucleus, and up to 325 cP in mitochondria [12]. Given the calibration curve takes the shape of a power law, it should be noted that a small irradiation-induced change in lifetime can potentially introduce a large error in determination of viscosity in viscous organelles such as mitochondria,

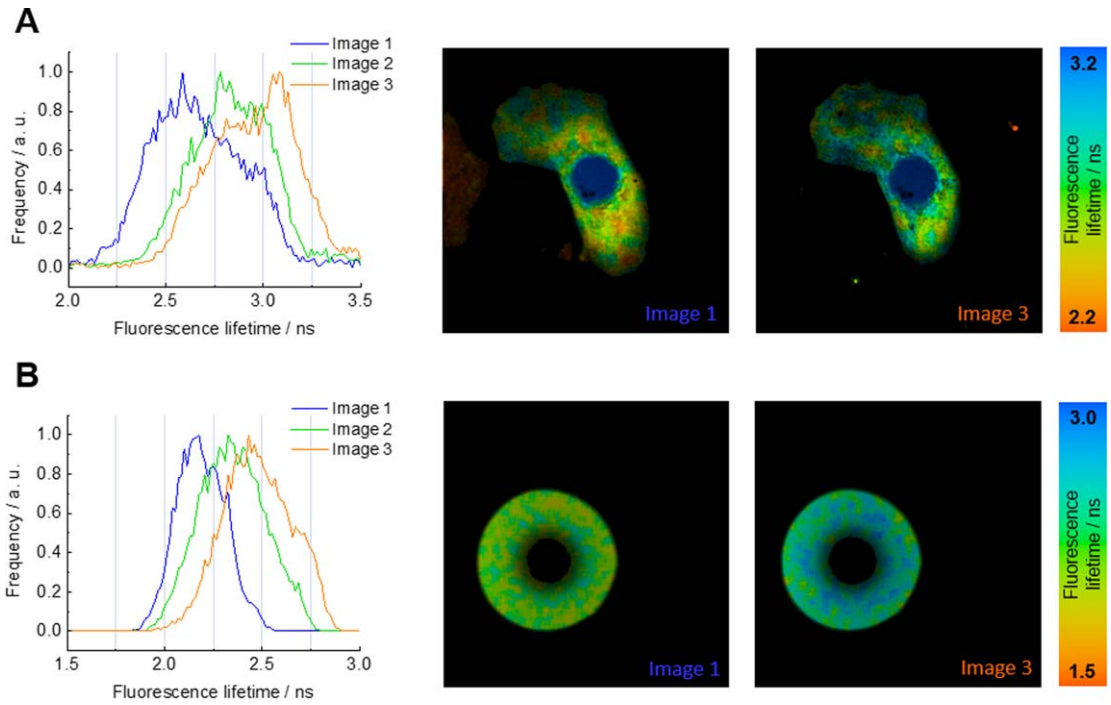

Figure 7. (A) Fluorescence lifetime increase in consecutive FLIM images induced by <1 mW 930 nm irradiation of a COS7 cell expressing the ER construct of BODIPY-HaloTag **1**. Left: fluorescence lifetime histograms obtained upon 15 min (image 2) and 25 min total (image 3) of irradiation. Images 1 and 3 are shown on the right. (B) Fluorescence lifetime increase upon 3 mW irradiation of Ni-NTA beads decorated with BODIPY-HaloTag **1**; Left: fluorescence lifetime histograms obtained upon 3 min (image 2) and 6 min total (image 3) of irradiation. Images 1 and 3 are shown on the right.

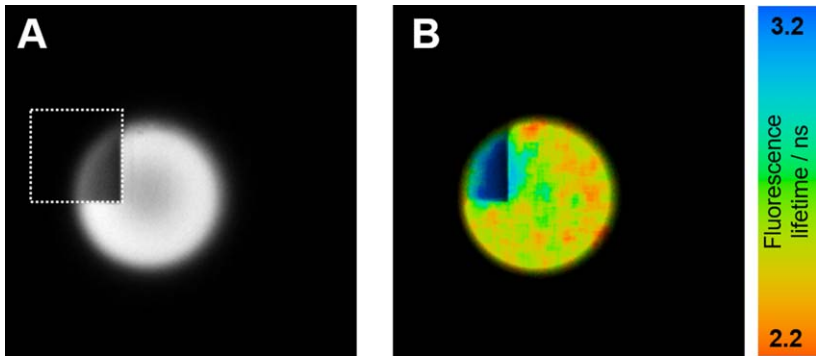

Figure 8. Two photon intensity (A) and FLIM (B) images of a Ni-NTA bead decorated with immobilised BODIPY-HaloTag **1**. The irradiation has resulted in a significant intensity decrease (A) and an increase in fluorescence lifetime (B) only in the irradiated section of the bead. The irradiated region is shown as a white dashed rectangle in (A).

while the values in the nucleus/cytosol will not be significantly affected.

To investigate the role of intracellular factors on the excitation-dependent lifetime changes of BODIPY-HaloTag **1**, we examined the irradiation of BODIPY-HaloTag **1** isolated on Ni-NTA beads, in the absence of intrinsic cellular milieu capable of (photo) redox processes. We observed the same effect of irradiation-induced increase in fluorescence lifetime even in the absence of cells (figure 7(B)). This indicates that the effect was intrinsic to BODIPY-HaloTag **1** and not due to a biophysical change in living cells induced by laser irradiation, or redox characteristics of the cellular environment.

Interestingly, when only a small part of the beads with immobilised BODIPY-HaloTag **1** was irradiated, the fluorescence lifetime had increased only in the irradiated region (figure 8), confirming the irradiation-induced photodamage of BODIPY-HaloTag **1**. Figure 8 also demonstrates significant photobleaching caused by irradiation. In contrast, when a small region of a cell was irradiated (as was done in figure 6), a subsequent lower magnification image revealed that fluorescence lifetime throughout the cell had increased significantly, whilst surrounding cells were not affected. We attribute this observation to diffusion of the photodamaged BODIPY-HaloTag **1** throughout the irradiated cell [23]. By contrast, such diffusion is

not possible when HaloTag protein is immobilised on a Ni-NTA bead. The effect of irradiation was remarkable and deemed **1** extremely difficult to work with for rigorous investigations of microviscosity changes via fluorescence lifetime measurement, in particular in live cells.

We performed MD simulations of BODIPY-HaloTag **1** to attempt to unravel the reasons behind the irradiation-dependent degradation of **1**, which was evidently absent in **2**. The results of our simulations are presented in supplementary videos 1 and 2 and the prevalent rotor-amino acid contacts for both rotors are summarised in table S1 together with percentage contact time out of a total trajectory time of approximately 400 ns each. The excited state of the BODIPY fluorophore is both a better oxidant and a reductant (compared to the ground state BODIPY), by 2.48 eV (photon energy corresponding to 500 nm). We therefore speculate that the irradiation-induced changes were likely caused by electron transfer between the excited state of our BODIPY probe and a site on the surface of a HaloTag protein. Literature data indicates that tryptophan and tyrosine residues are likely to quench BODIPY excited state [24]. While our computational modelling (table S1) did not reveal any tryptophan or tyrosine residues that are exclusively in contact with **1**, there is a significant number of amino-acids such as G40, Q165, N166, E170, P174, R179, P180, L181, T182, E183, M186 and R190 including charged amino-acids E170, R179, E183 and R190, that are in contact with **1** but never come into contact with **2** (table S1). Reduced fluorescence lifetime of our probe upon irradiation is consistent with a dynamic quenching mechanism. The reduced intensity upon irradiation points at the irreversibility of this excited state reaction (i.e. it proceeds to products with the removal of fluorescent BODIPY molecules).

This unexpected consequence of a slightly altered linker length highlights the fact that photophysical properties of any new probe have to be carefully taken into account, before its practical applications are possible. This is especially true for studies in which a molecular rotor is found in the close vicinity of a protein, as the local protein environment may significantly affect the rotor's photophysics [25]. In such cases, careful control and calibration measurements are required prior to quantitative studies. Based on our data we conclude that rotor **1** with the longer linker is unsuitable for microviscosity imaging, while rotor **2** is an excellent candidate for intracellular viscosity mapping at organelle level.

3. Conclusions

Two BODIPY-based ligands were designed for measuring microviscosity in cellular organelles by binding to HaloTag proteins expressed in the subcellular compartment of interest. Both ligands were able to penetrate cells, specifically label the desired intracellular location, and quantitatively determine the microviscosity of that particular environment via fluorescence lifetime imaging microscopy (FLIM).

Although the two ligands differed only slightly in the structure of the linker between molecular rotor and HaloTag recognition motif, one of them was significantly affected by photo-induced damage when bound to the HaloTag protein, while the other dye showed no changes upon irradiation. Excitation by laser light resulted in a gradual increase of fluorescence lifetime of BODIPY-HaloTag **1**, whereas the fluorescence lifetime of BODIPY-HaloTag **2** was stable under similar imaging conditions. Irradiation-induced electron transfer between the BODIPY moiety and the HaloTag protein was deemed as a plausible explanation for the photostability issue of BODIPY-HaloTag **1**. Our results demonstrate that when molecular rotors are directed to organelles of interest via genetic targeting, it is essential to characterise the probe in the protein-bound state, both *in vitro* and *in cellulo,* since binding to the targeted protein may significantly alter the probe's photophysical behaviour.

Fluorescence microscopy is the major toolbox of cell biologists and a great number of fluorescent probes have been developed for quantifying parameters of the cellular microenvironment using FLIM. Unfortunately, the fluorescence lifetime of environment sensing fluorophores may be affected by photodegradation of the probe. Investigating the photostability is essential for obtaining reliable results with environment sensing fluorophores such as molecular rotors in the complex and dynamic environment of live cells. Careful control measurements need to be performed to characterise microviscosity sensors against photodegradation and potential deleterious effects on cells, such as release of reactive oxygen species. Only upon such scrutiny can the fluorescence lifetime of these probes be used for quantifying physically and chemically induced dynamic changes of microviscosity and to apply them as tools for studying questions in biology and medicine.

4. Methods

4.1. BODIPY-HaloTag ligand synthesis

Ligand **2** was synthesised as reported previously [12]. For the synthesis of ligand **1**, O4 linker HaloTag amine ligand (Promega, US) was dissolved in anhydrous DMSO (0.5 mg in 100 μl). BODIPY-NHS was dissolved in anhydrous DMSO. DIPEA was incubated with O4 linker HaloTag amine ligand to a final concentration of 39.15 mM before addition of NHS-BODIPY to a final concentration of 4.35 mM and incubation at 25 °C for 16 h. Unreacted HaloTag amine ligand was quenched with excess glycine. Ligands were assessed by by ElectroSpray Ionization mass spectrometry (figure S5).

4.2. Protein expression and labelling with BODIPY ligands

HaloTag protein was expressed using a pET30a-HaloTag plasmid reported previously [12]. *Escherichia coli* transformed with pET30a-HaloTag were induced with 1 mM IPTG at an optical density of 0.6 at 600 nm. Cells were harvested 6 h post induction. Bacterial pellets were lysed in 50 mM Tris-HCl, pH 7.5, 500 mM NaCl, 0.2% Triton X-100, 10% glycerol, 20 mM imidazole, 0.2 mM PMSF and cOmplete™ EDTA-free protease inhibitor cocktail (Roche, US)) using an EmulsiFlex-C3 homogeniser (AVESTIN, Canada). Lysate was centrifuged at 20 000 g for 30 min before addition of 1 ml Ni-NTA beads (QIAGEN) and incubation for 2 h at 4 °C. Beads were washed five times with 20 ml lysis buffer supplemented with 30 mM imidazole. Protein was eluted with 500 mM imidazole in lysis buffer without Triton X-100 before buffer exchange into HKM buffer (150 mM KCl, 50 mM HEPES, pH 7.5, and 10 mM $MgCl_2$) by dialysis. 222 μM HaloTag protein was incubated with 414 μM ligand **1** or **2** for 16 h to generate BODIPY-HaloTag **1** and **2**, respectively. Free ligand was separated from BODIPY-HaloTag by gel filtration using a Centri Pure P2 Zetadex column (Generon. Berks, UK).

4.3. Bead functionalisation

Beads functionalised with BODIPY-HaloTag **1** were prepared by incubating 10 μl of 50 μM purified BODIPY-HaloTag with 10 μl of Ni-NTA beads in 500 μl of HKM buffer for 10 min at room temperature. Beads were pelleted by centrifugation at 5000 g for 1 min, supernatant containing unbound ligand **1** was removed and beads were washed twice in 1 ml of HKM before transfer to an 8-well chamber slide (LabTekII Chamber Coverglass) for imaging.

4.4. *In vitro* calibration of BODIPY-HaloTag ligand 1

BODIPY-HaloTag **1** was calibrated in water/glycerol mixtures as previously described for BODIPY-HaloTag **2** [12]. Briefly, BODIPY-HaloTag **1** was incubated in water/glycerol mixtures at 10 °C, 20 °C, 30 °C, and 40 °C, spanning a range of viscosities between *ca* 1–7000 cP. Solutions were transferred to 8-well chamber slides (LabTekII Chamber Coverglass) and time-resolved fluorescence measurements were performed to generate fluorescence lifetime/viscosity calibration curves as described previously [12].

4.5. Mammalian cell culture and HaloTag transfection

COS7 cells (Sigma-Aldrich, UK) were cultured in Dulbecco's modified Eagle's medium with 4500 mg l^{-1} glucose (Sigma-Aldrich, UK) supplemented with 10% Fetal Calf Serum. pFLAG-CMV1 HaloTag expression vectors were described previously [12]. Transfections were carried out with a Neon Transfection System (Invitrogen, Paisley, UK). 1.5 μg of HaloTag mammalian expression vector was mixed with 3×10^5 cells prior to electroporation, 48 h prior to imaging.

4.6. Image acquisition

Confocal images were acquired using a Zeiss 780 confocal microscope. Time-resolved fluorescence decays were collected using time-correlated single-photon counting (TCSPC) As described previously [12]. BODIPY was excited using a mode-locked femtosecond Ti:Sapphire laser (Coherent, Chameleon Vision II) using two photon excitation at 930 nm (140 fs pulse duration, 80 MHz). Fluorescence lifetime imaging microscopy (FLIM) was performed using a Leica, SP5 II confocal laser scanning microscope. Fluorescence was collected between 500 and 580 nm using a PMC-100-1 photomultiplier tube (Hamamatsu) and an SPC-830 single-photon counting card (Becker-Hickl). Live cell imaging was performed in glass bottom 8-well chamber slides (Nunc™, Lab-Tek, Thermofisher, MA. US.). Cells were seeded at approximately 1×10^4 cells per 0.7 cm^2 surface area chamber. Prior to imaging, cells were labelled for 30 min with 100 nM BODIPY ligand in PBS supplemented with $MgCl_2$ and $CaCl_2$ at 37 °C prior to three washes with PBS. Cells were imaged in FluoroBrite™ Dulbecco's modified Eagle's medium with 4500 mg l^{-1} glucose (Gibco™ Thermofisher, MA. US.).

4.7. FLIM analysis

FLIM analysis was performed as described previously [12]. Multi-exponential fitting was carried out using SPCI software (Becker-Hickl) with the nonlinear least squares method and reconvolution algorithm for finding the best fit. χ^2 value and randomness of residuals was used to judge goodness of fit. Decay models of fluorescence for HaloTag bound BODIPY ligands were judged to be bi-exponential and followed the equation

$$I(t) = \sum_{i-1}^{n} \alpha_i \exp(-t/\tau_i)$$

where I is fluorescence intensity, t is time, and α_i are the amplitudes and τ_i the fluorescence lifetimes of the n exponentially decaying components. Mean fluorescence lifetime was calculated using the following equation:

$$\tau_{avg} = \frac{\sum \alpha_i \tau_i^2}{\sum \alpha_i \tau_i}$$

4.8. Molecular dynamics simulations

Models of the BODIPY-HaloTag **1** and **2** were constructed based on the parameters described in our previous work [12], with the linker of ligand **1** comprising of 3 PEG units and the linker of ligand **2**

comprising only a single PEG unit. Both systems were solvated in approximately 11 000 molecules of TIP4P-2005 [26] water and neutralized by addition of sodium and chlorine counter-ions to a total salt concentration of 0.15 M. After minimization, both systems were equilibrated in the NpT ensemble at 300 K and a pressure of 1.0 bar. Bonds to hydrogen were constrained to enable a 2 fs integration time step for simulation. Electrostatics were described using the particle mesh Ewald procedure. Nonboned and electrostatic cutoffs were set at 1.2 nm. Position restraints for equilibration were set at 1000 kJ A^{-2}. Subsequent to equilibration, production simulations of 400 ns were performed for each system and frames were saved every 0.5 ns for analysis. Based on the result of these simulations, contacts between the BODIPY molecule and the HaloTag protein were identified in each frame using *mdmat* from the GROMACS software suite [27]. For each identified contact, the amount of time it is present during the simulation was calculated and expressed as a percentage (table S1). The contacts were also mapped to the surface of the HaloTag protein (figure 3).

Acknowledgments

JEC was funded by the MRC (MCMB MR/R009120/1) and the Alpha-1 Foundation (Award ID 395467). MK was funded by an Imperial College President's PhD Scholarship and an EPSRC Doctoral Prize Fellowship. RGH and PJB were funded by A*STAR. SJM was funded by the BLF, the MRC, the Alpha-1 Foundation and Cambridge NIHR BRC. MKK is grateful for the EPSRC for Career Acceleration Fellowship (EP/I003983/1). The authors have declared that no conflicting interests exist.

ORCID iDs

Markéta Kubánková https://orcid.org/0000-0001-7086-8938
Joseph E Chambers https://orcid.org/0000-0003-4675-0053
Roland G Huber https://orcid.org/0000-0001-5093-5988
Peter J Bond https://orcid.org/0000-0003-2900-098X
Stefan J Marciniak https://orcid.org/0000-0001-8472-7183
Marina K Kuimova https://orcid.org/0000-0003-2383-6014

References

[1] Kao H P, Abney J R and Verkman A S 1993 Determinants of the translational mobility of a small solute in cell cytoplasm *J. Cell Biol.* **120** 175–84
[2] Haidekker M A and Theodorakis E A 2007 Molecular rotors–fluorescent biosensors for viscosity and flow *Org. Biomol. Chem.* **5** 1669–78
[3] Kuimova M K 2012 Mapping viscosity in cells using molecular rotors *Phys. Chem. Chem. Phys.* **14** 12671–86
[4] Vyšniauskas A and Kuimova M K 2018 A twisted tale: measuring viscosity and temperature of microenvironments using molecular rotors *Int. Rev. Phys. Chem.* **37** 259–85
[5] Zhao M, Zhu Y, Su J, Geng Q, Tian X, Zhang J, Zhou H, Zhang S, Wu J and Tian Y 2016 A water-soluble two-photon fluorescence chemosensor for ratiometric imaging of mitochondrial viscosity in living cells *J. Mater. Chem.* B **4** 5907–12
[6] Yang Z *et al* 2013 A self-calibrating bipartite viscosity sensor for mitochondria *J. Am. Chem. Soc.* **135** 9181–5
[7] Yang Z, He Y, Lee J H, Chae W-S, Ren W X, Lee J H, Kang C and Kim J S 2014 A Nile Red/BODIPY-based bimodal probe sensitive to changes in the micropolarity and microviscosity of the endoplasmic reticulum *Chem. Commun.* **50** 11672–5
[8] Lee H, Yang Z, Wi Y, Kim T W, Verwilst P, Lee Y H, Han G-I, Kang C and Kim J S 2015 BODIPY-coumarin conjugate as an endoplasmic reticulum membrane fluidity sensor and its application to ER stress models *Bioconjug. Chem.* **26** 2474–80
[9] Kubánková M, López-Duarte I, Kiryushko D and Kuimova M K 2018 Molecular rotors report on changes in live cell plasma membrane microviscosity upon interaction with beta-amyloid aggregates *Soft Matter* **14** 9466–74
[10] Wang C, Song X, Chen L and Xiao Y 2016 Specifically and wash-free labeling of SNAP-tag fused proteins with a hybrid sensor to monitor local micro-viscosity *Biosens. Bioelectron.* **89** 757–64
[11] Gatzogiannis E, Chen Z, Wei L, Wombacher R, Kao Y-T, Yefremov G, Cornish V W and Min W 2012 Mapping protein-specific micro-environments in live cells by fluorescence lifetime imaging of a hybrid genetic-chemical molecular rotor tag *Chem. Commun.* **48** 8694–6
[12] Chambers J E, Kubánková M, Huber R G, López-Duarte I, Avezov E, Bond P J, Marciniak S J and Kuimova M K 2018 An optical technique for mapping microviscosity dynamics in cellular organelles *ACS Nano* **12** 4398–407
[13] Kuimova M K, Yahioglu G, Levitt J A and Suhling K 2008 Molecular rotor measures viscosity of live cells via fluorescence lifetime imaging *J. Am. Chem. Soc.* **130** 6672–3
[14] Kubánková M, López-Duarte I, Bull J A, Vadukul D M, Serpell L C, de Saint Victor M, Stride E and Kuimova M K 2017 Probing supramolecular protein assembly using covalently attached fluorescent molecular rotors *Biomaterials* **139** 195–201
[15] Woodcock E M, Girvan P, Eckert J, Duarte I L, Kubánková M, van Loon J J W A, Brooks N J and Kuimova M K 2019 Measuring intracellular viscosity in conditions of hypergravity *Biophys. J.* **116** 1984–93
[16] Vyšniauskas A, Qurashi M, Gallop N, Balaz M, Anderson H L and Kuimova M K 2015 Unravelling the effect of temperature on viscosity-sensitive fluorescent molecular rotors *Chem. Sci.* **6** 5773–8
[17] Los G V *et al* 2008 HaloTag: a novel protein labeling technology for cell imaging and protein analysis *ACS Chem. Biol.* **3** 373–82
[18] Oesterhelt F, Rief M and Gaub H E 1999 Single molecule force spectroscopy by AFM indicates helical structure of poly (ethylene-glycol) in water *New J. Phys.* **1** 6–6
[19] Förster T and Hoffmann G 1971 Die Viskositätsabhängigkeit der Fluoreszenzquantenausbeuten einiger Farbstoffsysteme *Zeitschrift für Phys. Chemie* **75** 63–76
[20] Vyšniauskas A, López-Duarte I, Thompson A J, Bull J A and Kuimova M K 2018 Surface functionalisation with viscosity-sensitive BODIPY molecular rotor *Methods. Appl. Fluoresc.* **6** 34001
[21] König K, So P T C, Mantulin W W and Gratton E 1997 Cellular response to near-infrared femtosecond laser pulses in two-photon microscopes *Opt. Lett.* **22** 135

[22] Jiménez-Banzo A, Nonell S, Hofkens J and Flors C 2008 Singlet oxygen photosensitization by EGFP and its chromophore HBDI *Biophys. J.* **94** 168–72
[23] Dickens J A *et al* 2016 The endoplasmic reticulum remains functionally connected by vesicular transport after its fragmentation in cells expressing Z-α1-antitrypsin *FASEB J.* **30** 4083–97
[24] Marmé N, Knemeyer J-P, Sauer M and Wolfrum J 2003 Inter- and intramolecular fluorescence quenching of organic dyes by tryptophan *Bioconjug. Chem.* **14** 1133–9
[25] Nguyen B, Ciuba M A, Kozlov A G, Levitus M and Lohman T M 2019 Protein environment and DNA orientation affect protein-induced Cy3 fluorescence enhancement *Biophys. J.* **117** 66–73
[26] Abascal J L F and Vega C 2005 A general purpose model for the condensed phases of water: TIP4P/2005 *J. Chem. Phys.* **123** 234505
[27] Berendsen H J C, van der Spoel D and van Drunen R 1995 GROMACS: a message-passing parallel molecular dynamics implementation *Comput. Phys. Commun.* **91** 43–56